molecular pharmaceutics

Article

pubs.acs.org/molecularpharmaceutics

Novel ^{19}F Activatable Probe for the Detection of Matrix Metalloprotease-2 Activity by MRI/MRS

Xuyi Yue,[†,‡,⊥,#] Zhe Wang,[†,⊥] Lei Zhu,[†,‡] Yu Wang,[†,§] Chunqi Qian,[∥] Ying Ma,[†] Dale O. Kiesewetter,*[,†] Gang Niu,[†] and Xiaoyuan Chen*[,†]

[†]Laboratory of Molecular Imaging and Nanomedicine (LOMIN), National Institute of Biomedical Imaging and Bioengineering (NIBIB), National Institutes of Health (NIH), Bethesda, Maryland 20892, United States

[‡]State Key Laboratory of Molecular Vaccinology and Molecular Diagnostics & Center for Molecular Imaging and Translational Medicine, School of Public Health, Xiamen University, Xiamen 361102, China

[§]Jiangsu Key Laboratory of Molecular and Functional Imaging, Department of Radiology, Zhongda Hospital, Medical School of Southeast University, Nanjing 210009, China

[∥]Laboratory of Functional and Molecular Imaging, National Institute of Neurological Disorders and Stroke (NINDS), National Institutes of Health, Bethesda, Maryland 20892, United States

ABSTRACT: Matrix metalloproteases (MMPs) have been found to be highly expressed in a variety of malignant tumor tissues. Noninvasive visualization of MMP activity may play an important role in the diagnosis of MMP associated diseases. Here we report the design and synthesis of a set of fluorine-19 dendron-based magnetic resonance imaging (MRI) probes for real-time imaging of MMP-2 activity. The probes have the following features: (a) symmetrical fluorine atoms; (b) the number of fluorine atoms can be increased through facile chemical modification; (c) readily accessible peptide sequence as the MMP-2 substrate; (d) activatable ^{19}F signal (off/on mode) via paramagnetic metal ion incorporation. Following optimization for water solubility, one of the probes was selected to evaluate MMP-2 activity by ^{19}F magnetic resonance spectroscopy (MRS). Our results showed that the fluorine signal increased by 8.5-fold in the presence of MMP-2. The specific cleavage site was verified by mass spectrometry. The selected probe was further applied to detect secreted MMP-2 activity of living SCC7 squamous cell carcinoma cells. The fluorine signal was increased by 4.8-fold by MRS analysis after 24 h incubation with SCC7 cells. This type of fluorine probe can be applied to evaluate other enzyme activities by simply tuning the substrate structures. This symmetrical fluorine dendron-based probe design extends the scope of the existing ^{19}F MRI agents and provides a simple but robust method for real-time ^{19}F MRI application.

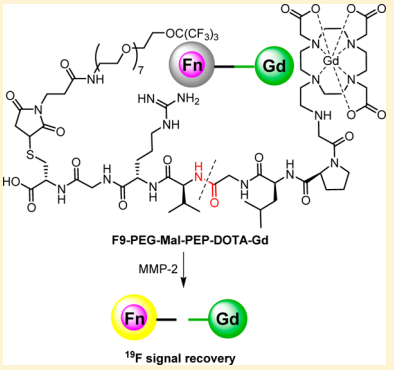

KEYWORDS: *^{19}F magnetic resonance imaging, ^{19}F magnetic resonance spectroscopy, activatable probe, matrix metalloproteases*

INTRODUCTION

Matrix metalloproteases (MMPs) are a family of endopeptidases composed of over 25 enzymes that require zinc or calcium to express their catalytic activities.[1,2] MMPs take part in a set of biological functions such as extracellular matrix degradation and remodeling, and bioactive molecules processing and release.[3] In normal tissues, the expression of active MMPs is low due to strict control mechanisms, whereas MMPs are overexpressed in numerous pathological diseases, such as inflammation, and tumor metastasis.[4]

Among the MMPs, the gelatinase subfamily including MMP-2 and MMP-9 have received great attention in the development of anticancer drugs.[5,6] Furthermore, augmented expression and activity of MMP-2 has been found in a variety of malignant tumor tissues of various organs.[7] Studies have shown that many types of diseases, such as cancer,[8] diabetes,[9,10] and hypertension,[11,12] are accompanied by elevated blood level of MMP-2.

Noninvasive visualization of activated MMPs has been a hot pursuit in recent years. Different imaging modalities, including optical imaging,[13−17] iron oxide-based magnetic resonance imaging (MRI),[18−22] and positron emission tomography,[23,24] were developed in recent years for the detection of protease activity with promising results. While different imaging strategies are complementary, optical imaging is the most widely studied approach to detect protease activity *in vivo*. Protease activatable near-infrared fluorescent probes that are specifically cleaved by MMPs to produce fragments with altered fluorescence have been reported both in chemical conjugates and in nanoparticle platforms.[13−17] However, optical imaging has limited translational potential into clinical practice due to

Received: June 23, 2014
Revised: August 19, 2014
Accepted: October 1, 2014
Published: October 1, 2014

the shallow penetration of the excitation/emission light, and the scattering of light in living subjects.[25]

^{19}F magnetic resonance imaging (^{19}F MRI) is a promising quantitative imaging technique. ^{19}F nuclide has 100% natural isotopic abundance with similar sensitivity to ^{1}H. Notably, negligible endogenous ^{19}F background in biological systems makes ^{19}F MRI an ideal modality to monitor protease activity,[26−29] track immune cells,[30] and quantitatively evaluate neovascular expansion using a clinical scanner.[31] Most current ^{19}F imaging agents are based on perfluorocarbon emulsions. Perfluoro-15-crown-5-ether (PFCE) is the most commonly used fluorous agent in ^{19}F MRI,[32] but PFCE is insoluble in most solvents and is not amenable to chemical modifications. Because of the potential importance of ^{19}F MRI for disease diagnosis, new ^{19}F probe design strategies are needed for real-time imaging of biological events to overcome the shortcomings of perfluorocarbon formulation. To this end, we designed and synthesized a set of probes with symmetrical fluorine moiety to detect MMP-2 activity. Our probe features tunable fluorine content while retaining its symmetrical structure and a single fluorine resonance. Furthermore, our activatable probe was able to detect MMP-2 activity through observation of increased ^{19}F signal intensity by magnetic resonance spectroscopy (MRS) and magnetic resonance imaging (MRI) upon exposure to the enzyme.

EXPERIMENTAL SECTION

Reagents and Instrumentation. Unless otherwise stated, all chemicals were used as received, and the reactions were monitored by analytical thin layer chromatography (TLC), on Merck precoated silica gel 60 F254 plates with visualization by ultraviolet irradiation at λ = 254 nm or staining with $KMnO_4$. Purifications were performed by silica gel chromatography. Intermediate peptide **10** CGRVGLPG-DOTA was synthesized on an automatic peptide synthesizer (CS Bio Co., Menlo Park, CA. DOTA is 1,4,7,10-tetraazacyclododecane-1,4,7,10-tetraacetic acid) by fluorenylmethoxycarbonyl (Fmoc) chemistry at a 1 mmol scale using a Gly-2-ClTrt resin. ^{1}H, ^{19}F, and ^{13}C NMR spectra were carried out on a Bruker 300 MHz NMR spectrometer, equipped with a $^{1}H/^{19}F/^{13}C$ 5 mm broad band probe. The ^{1}H, ^{19}F, and ^{13}C NMR spectra were recorded at 300, 282, and 75.5 MHz, respectively. Mass analysis was conducted on a Waters LC−MS system (Waters, Milford, MA) that included an Acquity UPLC unit coupled to the Waters Q-Tof Premier high-resolution mass spectrometer.

Chemistry. *2-(2-(2-(2-Hydroxyethoxy)ethoxy)ethoxy)ethyl 4-Methylbenzenesulfonate, **2**.* *p*-Toluenesulfonyl chloride (TsCl) (11.4 g, 60 mmol) was added to a mixture of tetraethylene glycol (21 mL, 23.4 g, 120.6 mmol), Et_3N (12.6 mL, 90 mmol), and DMAP (0.72 g, 6 mmol) in anhydrous CH_2Cl_2 (300 mL) at 0 °C in one portion. The reaction mixture was then stirred at room temperature (rt) overnight. H_2O was added to quench the reaction, and the mixture was then extracted with CH_2Cl_2. Removing the combined solvent under vacuum followed by silica gel flash chromatography using CH_2Cl_2/MeOH (20/1) as the eluent afforded compound **2** (13.1 g, 63% yield) as a yellow oil. ^{1}H NMR (300 MHz, $CDCl_3$) δ 7.70−7.67 (m, 2H), 7.28−7.24 (m, 2H), 4.07−4.04 (m, 2H), 3.60−3.54 (m, 6H), 3.53−3.51 (m, 2H), 3.50−3.46 (m, 6H), 3.03 (br, 1H), 2.34 (s, 3H).

*2-(2-(2-(2-Azidoethoxy)ethoxy)ethoxy)ethanol, **3**.* To a solution of tetraethylene glycol monotosylate **2** (13 g, 37.4 mmol) in DMF (200 mL) was added sodium azide (3.6 g, 56 mmol) carefully. The reaction mixture was stirred at 60 °C overnight. After the solution was cooled to rt, water was added slowly to dissolve minor remaining solid. The mixture was then extracted with ethyl acetate. The combined organic mixture was washed successively with water and brine and concentrated by rotary evaporation. The residue was purified by silica gel column chromatography using CH_2Cl_2/MeOH (20/1) as the eluent to afford compound **3** (6.9 g, 84% yield) as a light yellow oil. ^{1}H NMR (300 MHz, $CDCl_3$) δ 3.76−3.59 (m, 12H), 3.57−3.54 (m, 2H), 3.36−3.33 (m, 2H), 2.91 (br, 1H).

*2-(2-(2-(2-Azidoethoxy)ethoxy)ethoxy)ethyl 4-Methylbenzenesulfonate, **4**.* To the azide compound **3** (9.32 g, 42.6 mmol) in CH_2Cl_2 (200 mL) was added Et_3N (8.4 mL, 60.0 mmol), *p*-toluenesulfonyl chloride (11.4 g, 59.9 mmol) successively 0 °C, the mixture was stirred overnight at rt. The mixture was poured into water, and the organic layer was separated and evaporated through rotary evaporation. The residue was purified by silica gel column chromatography using hexane/EtOAc (1/1) as the eluent to afford compound **4** (7.6 g, 93% yield) as a light yellow liquid. ^{1}H NMR (300 MHz, $CDCl_3$) δ 7.82−7.78 (m, 2H), 7.36−7.33 (m, 2H), 4.17−4.14 (m, 2H), 3.67−3.58 (m, 8H), 3.59−3.58 (m, 4H), 3.40−3.37 (m, 2H), 2.45 (s, 3H).

*23-Azido-3,6,9,12,15,18,21-heptaoxatricosan-1-ol, **5**.* To a suspension of 60% sodium hydride (1.6 g, 40 mmol) in 90 mL of anhydrous THF at 0 °C was added tetraethylene glycol **1** (6.98 g, 3.6 mmol) in 20 mL of anhydrous THF dropwise under nitrogen. The reaction was stirred at 0 °C for 1 h and continued at rt for another 2 h. Tosylate **4** (6.7 g, 1.8 mmol) in THF (20 mL) was added dropwise to the refluxing solution of sodium alcoholate; then the mixture was refluxed for another 10 h. After cooling to rt, the mixture was quenched with H_2O carefully. Upon solvent evaporation, the residue was extracted with EtOAc, washed with H_2O, and saturated sodium chloride solution successively; the combined organic phase was concentrated through rotary evaporation and subjected to silica gel chromatography using CH_2Cl_2/MeOH as the eluent to afford compound **5** (5.2 g, 73% yield) as a clear oil. ^{1}H NMR (300 MHz, $CDCl_3$) δ 3.69−3.66 (m, 4H), 3.65−3.61 (m, 20H), 3.58−3.56 (m, 4H), 3.35 (t, J = 4.2 Hz, 4H), 2.62 (br, 1H).

*23-Azido-3,6,9,12,15,18,21-heptaoxatricosyl 4-methylbenzenesulfonate, **6**.* To the azide compound **5** (3 g, 7.6 mmol) in CH_2Cl_2 (35 mL) was added Et_3N (1.5 mL, 11 mmol), then *p*-toluenesulfonyl chloride (2.1 g, 11 mmol) was added in one portion at 0 °C; the reaction was stirred overnight at rt. The mixture was poured into water, and the organic layer was separated and evaporated through rotary evaporation. The residue was purified by silica gel column chromatography using hexane/EtOAc (1/1) as the eluent to afford compound **6** (3.2 g, 76% yield) as a light yellow liquid. ^{1}H NMR (300 MHz, $CDCl_3$) δ 7.62 (d, J = 8.1 Hz, 2H), 7.19 (d, J = 8.1 Hz, 2H), 4.00−3.97 (m, 2H), 3.52−3.48 (m, 24H), 3.47−3.40 (m, 4H), 3.21 (t, J = 5.1 Hz, 2H), 2.28 (s, 3H). ^{13}C NMR (75.5 MHz, $CDCl_3$) δ 144.5, 132.6, 129.5, 127.6, 70.3, 70.24, 70,22, 70.17, 70.10, 69.6, 69.1, 68.2, 50.3, 21.2.

*26-Azido-1,1,1-trifluoro-2,2-bis(trifluoromethyl)-3,6,9,12,15,18,21,24-octaoxahexacosane, **7**.* To the azide compound **6** (1.0 g, 1.8 mmol) in dry DMF (9 mL) was added sodium perfluoro-*tert*-butoxide (0.94 g, 3.6 mmol), which was prepared according to the literature.[33] The reaction mixture was stirred at 65 °C overnight, and H_2O was added to the cool down mixture. The mixture was extracted with EtOAc,

the pooled organic extracts were washed with water and brine, the combined organic phase was concentrated under reduced pressure through rotary evaporation, and the residue was purified by silica gel flash chromatography using hexane/EtOAc (1/1) as the eluent to afford compound **7** (0.78 g, 70% yield) as a clear liquid. ^{1}H NMR (300 MHz, $CDCl_3$) δ 4.11 (t, J = 4.8 Hz, 2H), 3.71−3.64 (m, 2H), 3.63−3.59 (m, 26H), 3.34 (t, J = 5.1 Hz, 2H). ^{19}F NMR (282 MHz, $CDCl_3$) δ 70.52. ^{13}C NMR (75.5 MHz, $CDCl_3$) δ 120.4 (q, J = 292.9 Hz), 80.8−79.3 (m), 71.1, 70.75, 70.73, 70.69, 70.64, 70.08, 69.44, 69.38, 69.36, 69.34, 69.32, 50.7. Mass (ESI) m/z 614.2 $[M + H]^+$.

26,26,26-Trifluoro-25,25-bis(trifluoromethyl)-3,6,9,12,15,18,21,24-octaoxahexacosan-1-amine, ***8****.* To the azide compound 7 (0.78 g, 1.3 mmol) in dry THF (10 mL) was added Ph_3P (0.6 g, 2.3 mmol). Upon the completion of the reaction as confirmed by TLC, water (0.23 mL) was added and the reaction continued overnight at rt. After removal of the solvent in vacuum, the residue was purified by silica gel column chromatography first using CH_2Cl_2/MeOH (16/1) then MeOH as the eluent to give compound **8** (0.7 g, 94% yield). ^{1}H NMR (300 MHz, $CDCl_3$) δ 4.00 (t, J = 4.5 Hz, 2H), 3.58 (t, J = 4.8 Hz, 2H), 3.50 (s, 24H), 3.39 (t, J = 5.4 Hz, 2H), 2.73 (br, 2H), 2.37 (br, 2H). ^{19}F NMR (282 MHz, $CDCl_3$) δ 70.68. ^{13}C NMR (75.5 MHz, $CDCl_3$) δ 120.1 (q, J = 295.2 Hz), 80.2−78.6 (m), 72.5, 70.9, 70.42, 70.36, 70.34, 70.31, 70.1, 69.2, 41.4. Mass (ESI) m/z 588.7 $[M + H]^+$.

3-(2,5-Dioxo-2,5-dihydro-1H-pyrrol-1-yl)-N-(26,26,26-trifluoro-25,25-bis(trifluoromethyl)-3,6,9,12,15,18,21,24-octaoxahexacosyl)propanamide, ***9*** *(F9-PEG-Mal).* To the amino compound **8** (235 mg, 0.4 mmol) in CH_2Cl_2 (4 mL) was added *N*,*N*-diisopropylethylamine (0.11 mL, 0.6 mmol); then 3-(maleimido)propionic acid *N*-hydroxysuccinimide ester (80 mg, 0.36 mmol) was added at 0 °C, and the mixture was stirred at rt for 4 h. The mixture was concentrated under vacuum, and the residue was purified by silica gel column chromatography using CH_2Cl_2/MeOH (16/1) as the eluent to afford compound **9** (196 mg, 73% yield). ^{1}H NMR (300 MHz, $CDCl_3$) δ 6.70 (s, 2H), 6.58 (br, 1H), 4.14 (t, J = 4.2 Hz, 2H), 3.84−3.79 (m, 2H), 3.74−3.70 (m, 2H), 3.64−3.59 (m, 24H), 3.53 (t, J = 5.1 Hz, 2H), 3.42−3.37 (m, 2H), 2.50 (t, J = 6.9 Hz, 2H). ^{19}F NMR (282 MHz, $CDCl_3$) δ 70.95. ^{13}C NMR (75.5 MHz, $CDCl_3$) δ 170.7, 170.2, 134.4, 120.4 (q, J = 297.5 Hz), 80.3−79.1 (m), 70.8, 70.7, 70.4, 69.83, 68.76, 68.4, 66.0, 65.6, 46.4, 39.6, 34.7, 34.6, 29.9. Mass (ESI) m/z 739.2 $[M + H]^+$.

Conjugation of DOTA Conjugated Peptide PEP-DOTA ***10*** *with F9-PEG-Mal* ***9****.* To the peptide **10** (253 mg, 0.22 mmol) in degassed PBS (150 mL) was added a solution of compound **9** (196 mg, 0.27 mmol) in degassed EtOH (30 mL). The mixture was stirred at rt under argon and monitored by analytical reversed-phase high performance liquid chromatography (RP-HPLC). The mixture was quenched by 0.1% aqueous TFA and concentrated through rotary evaporation. The residue was purified by preparative HPLC. The proper fraction was collected and lyophilized to afford fluorine-containing peptide as a white solid (316 mg, 76% yield). Mass (ESI) m/z 942.6 $[M + 2H]^{2+}$. ^{19}F NMR (282 MHz, D_2O) δ 70.50. For semipreparative HPLC, a Beckman Ultrasphere C_{18} column (10 × 250 mm) and a gradient elution profile were used with 0.5% phosphoric acid in water (solvent A) and 0.5% phosphoric acid in CH_3CN (solvent B). The elution profile was isocratic at 5% solvent B for 5 min, then a gradient to 80% solvent B over 45 min. The flow rate was 4 mL/min. The major peak at about 27.0 min was collected. The purity of the resulting compound was conducted by analytical HPLC.

Synthesis of Probe F9-PEG-Mal-PEP-DOTA-Gd, ***11****.* A DOTA-containing peptide (75 mg) was dissolved in PBS, $GdCl_3 \cdot 6H_2O$ (5 equiv) was added, and the pH of the solution was adjusted to 4−5. The mixture was heated at 80 °C, and the reaction was monitored by HPLC; typically the reaction was completed in 4 h. The mixture was centrifuged and subject to semipreparative HPLC. A Beckman Ultrasphere C_{18} column (10 × 250 mm) and a gradient elution profile were used with 0.5% phosphoric acid in water (solvent A) and 0.5% phosphoric acid in CH_3CN (solvent B). The gradient elution profile was from 5% solvent B to 80% solvent B in 50 min, then to 100% solvent over the next 5 min. The flow rate was 4 mL/min. The major peak at 34.4 min was collected and lyophilized. Analytical HPLC was used to confirm the purity (Condition: 4.6 × 150 mm Phenomenex C_{18} column, 1 mL/min, detection wavelength at 214 nm, elution profile, a gradient from 5% solvent B to 60% solvent B in 15 min, and to 100% solvent B over next 5 min). The retention time of the fluorinated peptide was 13.7 min. Mass (ESI) m/z 1019.6 $[M + 2H]^{2+}$.

1-Azido-34,34,34-trifluoro-30,30-bis(((1,1,1,3,3,3-hexafluoro-2-(trifluoromethyl)propan-2-yl)oxy)methyl)-33,33-bis(trifluoromethyl)-3,6,9,12,15,18,21,24,28,32-decaoxatetratriacontane, ***13****.* To a suspension of 60% sodium hydride (0.16 g, 4.0 mmol) in 10 mL of THF at 0 °C was added alcohol **12** (2.04 g, 2.4 mmol), which was prepared according to the reported procedure,[33] in 6 mL of anhydrous THF dropwise. The reaction was stirred at 0 °C for 1 h and then at rt for another 2 h. Tosylate **6** (1.1 g, 2.0 mmol) in THF (6 mL) was added dropwise to the refluxing solution of sodium alcoholate. The mixture continued to reflux at 70 °C for overnight. Upon being cooled to rt, the mixture was quenched with H_2O. After solvent evaporation, the residue was extracted with EtOAc, washed with H_2O, concentrated through rotary evaporation, and subjected to silica gel chromatography using hexane/EtOAc as eluent to afford compound **13** (1.05 g, 43% yield) as a clear oil. ^{1}H NMR (300 MHz, $CDCl_3$) δ 3.91 (s, 6H), 3.56−3.48 (m, 28H), 3.43−3.40 (m, 2H), 3.37−3.25 (m, 4H), 3.24−3.22 (m, 4H), 1.73−1.65 (m, 2H). ^{19}F NMR (282 MHz, $CDCl_3$) δ 71.00. ^{13}C NMR (75.5 MHz, $CDCl_3$) δ 120.1 (q, J = 292.9 Hz), 80.4−78.5 (m), 70.64, 70.61, 70.55, 70.45, 70.3, 70.2, 70.0, 68.5, 68.0, 65.7, 65.4, 50.6, 46.1, 29.6.

34,34,34-Trifluoro-30,30-bis(((1,1,1,3,3,3-hexafluoro-2-(trifluoromethyl)propan-2-yl)oxy)methyl)-33,33-bis(trifluoromethyl)-3,6,9,12,15,18,21,24,28,32-decaoxatetratriacontan-1-amine, ***14****.* To the azide compound **13** (0.8 g, 0.65 mmol) in dry THF (6 mL) was added Ph_3P (0.4 g, 1.5 mmol). The reaction was stirred overnight, and water (0.15 mL) was added. After the completion of the hydrolysis, the solvent was removed in vacuum through rotary evaporation; the residue was purified by silica gel column chromatography first using CH_2Cl_2/MeOH (16/1) then MeOH as the eluent to give compound **14** (0.62 g, 85% yield). ^{1}H NMR (300 MHz, $CDCl_3$) δ 3.98 (s, 6H), 3.62−3.56 (m, 24H), 3.51−3.49 (m, 4H), 3.45−3.36 (m, 4H), 3.31 (s, 2H), 2.97 (br, 2H), 2.86 (t, J = 4.8 Hz, 2H), 1.78 (t, J = 6.3 Hz, 2H). ^{19}F NMR (282 MHz, $CDCl_3$) δ 70.71. ^{13}C NMR (75.5 MHz, $CDCl_3$) δ 121.8 (q, J = 295.2 Hz), 82.1−80.1 (m), 71.52, 71.46, 71.41, 71.33, 71.30, 71.26, 71.22, 71.1, 70.9, 69.8, 69.2, 68.0, 67.1, 67.0, 47.6, 40.7, 31.0. Mass (ESI) m/z 1201.2 $[M + H]^+$.

3-(2,5-Dioxo-2,5-dihydro-1H-pyrrol-1-yl)-N-(34,34,34-trifluoro-30,30-bis(((1,1,1,3,3,3 hexafluoro-2-(trifluoromethyl)-

*propan-2-yl)oxy)methyl)-33,33-bis(trifluoromethyl)-3,6,9,12,15,18,21,24,28,32-decaoxatetratriacontyl)-propanamide, **15***. To a solution of compound **14** (150 mg, 0.11 mmol) in anhydrous DMF (1 mL) at 0 °C was added 3-maleimidopropionic acid (29 mg, 0.17 mmol), 1-hydroxybenzotriazole (HOBt) (23 mg, 0.17 mmol), 1-(3-(dimethylamino)-propyl)-3-ethylcarbodiimide hydrochloride (EDC·HCl) (33 mg, 0.17 mmol), 4 Å molecular sieves (100 mg), and DIPEA (30 μL, 0.17 mmol) successively. The mixture was stirred at 0 °C for 0.5 h and then at rt overnight. The mixture was quenched with ice water and extracted with CH_2Cl_2. The organic extracts were washed with water and brine successively. After drying the organic layer and evaporation of the solvent under vacuum, the residue was purified by silica gel column chromatography using CH_2Cl_2/MeOH to afford the product at 100 mg; 30 mg of starting material **14** was recovered (81% yield after recovery). ^{1}H NMR (300 MHz, $CDCl_3$) δ 6.70 (s, 2H), 6.42 (br, 1H), 4.03 (s, 6H), 3.86−3.71 (m, 2H), 3.65−3.62 (m, 26H), 3.57−3.52 (m, 4H), 3.50−3.42 (m, 6H), 3.36 (s, 2H), 2.52 (t, J = 7.2 Hz, 2H), 1.87−1.78 (m, 2H). ^{19}F NMR (282 MHz, $CDCl_3$) δ 70.52. ^{13}C NMR (75.5 MHz, $CDCl_3$) δ 170.6, 170.2, 134.4, 120.3 (q, J = 293.7 Hz), 80.2−79.0 (m), 70.70, 70.66, 70.4, 69.8, 68.8, 68.3, 65.9, 65.6, 46.3, 39.6, 34.6, 34.5, 29.8. Mass (ESI) m/z 1350.4 $[M + H]^+$.

Cell Culture Experiment. Squamous cell carcinoma cells (SCC7) were cultured in RPMI-1640 medium supplemented with 10% fetal bovine serum (FBS) (Hyclone) 100 μg/mL penicillin, and 100 U/mL streptomycin at 37 °C with 5% CO_2.

MMP-2 Concentration Determination. We collected cell culture medium supernatant to evaluate the capacity of the developed probe to detect the secreted MMP-2 by SCC7 cancer cells. Briefly, the monolayer of cultured cells were washed two times with ice cold PBS, followed by adding fresh complete cell culture medium 24 h prior to supernatant collection. The next day, the supernatant was harvested and centrifuged at 3000 rpm for 3 min to get rid of cell debris. The concentration of MMP-2 in the supernatant was quantified by MMP-2 ELISA assay (R&D) following the manufacturer's protocol.

^{19}F NMR and Imaging. The probe was added to MMP-2 buffer (26.9 nM) or SCC7 cell medium (1% 2,2,2-trifluoroethanol with 5% D_2O); the final concentration of the probe is 0.25 mM. The mixture was put into an NMR tube and incubated at 37 °C. ^{19}F NMR was acquired at different time points using the same parameters. A broad spectrum pan-MMP inhibitor (100 μM) was added to the solution for control experiments. For ^{19}F NMR imaging, the experiments were performed with a home-built surface coil tuned to 281.65 MHz, which is the ^{19}F resonance frequency at 7 T. A 2D FLASH image was acquired on the fluorine-containing sample, with the following acquisition parameters: TE = 3 ms, TR = 100 ms, FOV = 4 × 4 cm^2, matrix size = 128 × 128, slice thickness = 2 mm, and FA = 30 deg.

RESULTS

Design of Probes. We synthesized a probe containing four specific segments. The first is the perfluorinated signal emitting portion **A**. This portion is somewhat tunable in that we are able to chemically synthesize a F9 or F27 moiety while maintaining the symmetry of ^{19}F signal. The unit **B** is a polyethylene glycol chain that enhances water solubility of the final construction. The unit **C** is a peptide substrate of MMP-2. The unit **D** is a chelated Gd^{3+} ion that serves as a signal modulator of the ^{19}F resonance due to its strong paramagnetic effect and shortening of transverse relaxation time (T_2). As constructed, the proximity of the Gd^{3+} to the ^{19}F resulted in significant attenuation of the ^{19}F signal. Upon MMP-2 incubation, the MMP substrate is site-specifically cleaved and the paramagnetic effect of Gd^{3+} toward ^{19}F is canceled, which induces the extension of T_2 and recovery of ^{19}F signal. The recovery rate of ^{19}F signal is proportional to the MMP-2 activity (Figure 1).

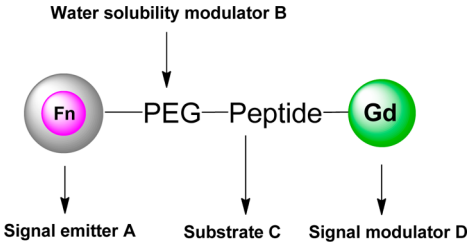

Figure 1. Schematic of ^{19}F-based MMP activatable probe. Fn represents fluorous unit with different numbers of symmetric fluorinated branches for signal emitter; PEG is poly(ethylene glycol).

Probe Synthesis and Characterization. The PEG linker was synthesized starting from commercially available tetraethylene glycol **1**. Selective protection of one of the hydroxyl groups with tosyl chloride afforded compound **2**; reaction of compound **2** with sodium azide gave compound **3**. A second tetraethylene glycol unit was linked to tosylate **4** to produce azide **5** with eight ethylene glycol units. Symmetrical F9 unit was introduced to the glycol linker by the S_N2 displacement of tosylate **6** with sodium per-fluoro-*tert*-butoxide. Reduction of azide **6** by the classical Staudinger reaction afforded free amine **8**. A maleimido group, for subsequent thiol conjugation, was introduced by the condensation of compound **8** with commercially available 3-(maleimido)propionic acid *N*-hydroxysuccinimide ester in high yield to give compound **9**. Compounds **7**−**9** exhibited single, sharp ^{19}F resonances with no loss of symmetry in the fluorinated unit.

Next we introduced the MMP-2 substrate into the PEGylated fluorinated unit. The MMP-2 cleavable peptide substrate **10**, Cys-Gly-Arg-*Val-Gly*-Leu-Pro-Gly-DOTA (abbreviated as PEP-DOTA), was synthesized by a standard solid-phase Fmoc peptide chemistry. The reaction between the free thiol group in peptide **10** and maleimido linker **9** proceeded smoothly with high yield. The ^{19}F signal modulator Gd^{3+} was introduced to the 1,4,7,10-tetraazacyclododecane-1,4,7,10-tetraacetic acid (DOTA) chelator in high efficiency (Scheme 1). The purity and identity of **11** were confirmed by analytical HPLC and LC−MS.

^{19}F-NMR Properties. Results by ^{19}F spectroscopy showed about 11 times difference in ^{19}F intensity before and after Gd^{3+} incorporation, indicating the strong paramagnetic effect of Gd^{3+} toward ^{19}F nuclei and the potential of this probe to detect enzyme activity.

Next we synthesized more highly branched probes with higher fluorine content. According to a reported strategy,[33] we synthesized alcohol **12** with 27 symmetrical fluorine atoms. Reaction of **12** with PEGlyated linker **6** afforded azide compound **13**. The azide was subjected to reduction to give free amine **14**, then condensation of amine **14** with 3-maleimidopropionic acid produced **15** (Scheme 2). All the synthesized compounds **12**−**15** showed single, sharp ^{19}F resonances. Next we attempted to attach F27 linker **15** to

Scheme 1. Synthesis of Activatable Probe F9-PEG-Mal-PEP-DOTA-Gd Containing 9 Symmetric Fluorine Atoms[a]

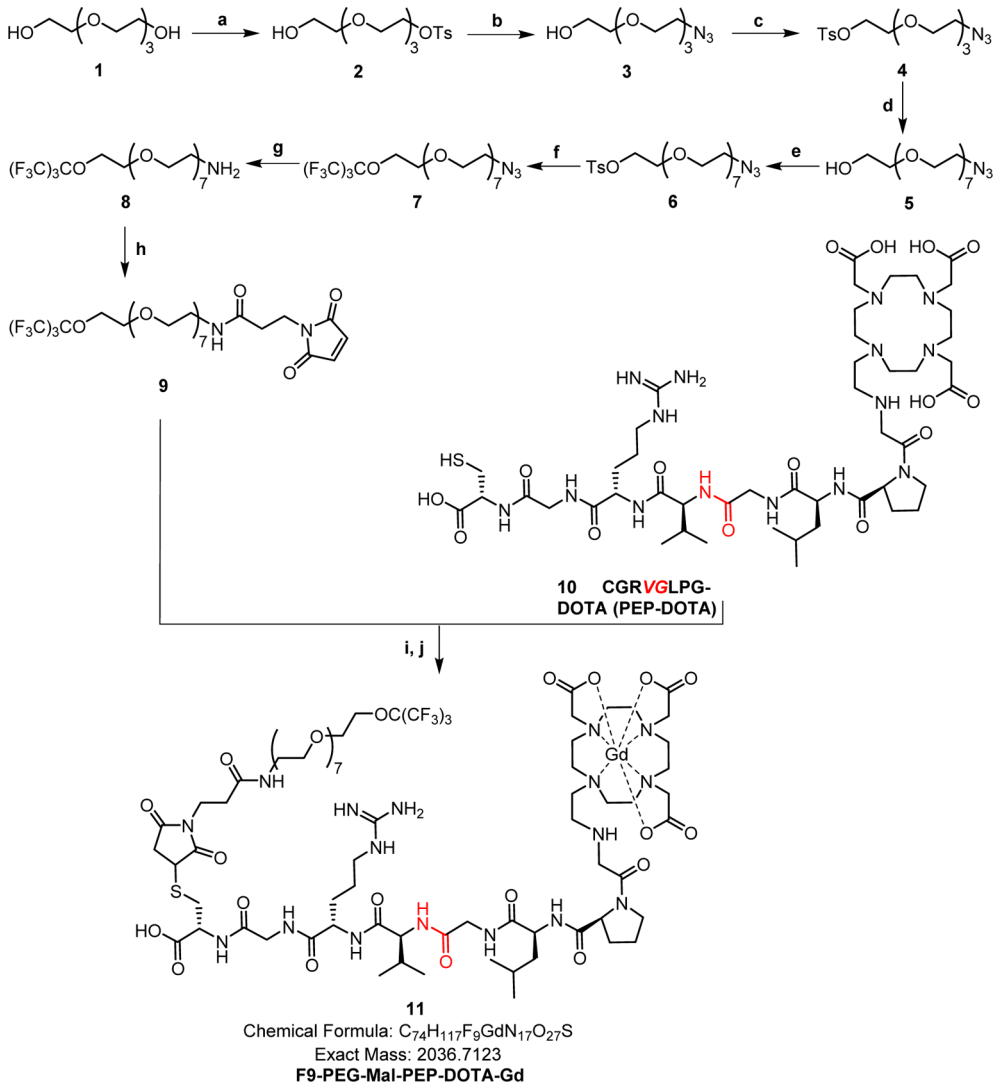

[a]Red color in compound **10** represents the specific cleavage site. Reagents and conditions: (a) TsCl, Et_3N, DCM, rt; (b) NaN_3, DMF, 65 °C; (c) TsCl, Et_3N, DCM; (d) tetraethylene glycol, NaH, THF, rt to reflux; (e) TsCl, Et_3N, THF; (f) $(CF_3)_3CONa$, DMF; (g) Ph_3P, THF, then H_2O, rt; (h) 3-(maleimido)propionic acid *N*-hydroxysuccinimide ester, DIPEA, DMF; (i) PBS/EtOH (v/v, 4/1), pH 7.4, rt; (j) $GdCl_3{\cdot}6H_2O$, PBS, pH 4–5, 80 °C.

Scheme 2. Synthetic Scheme Towards Activatable Probe Containing Symmetric 27 Fluorine Atoms[a]

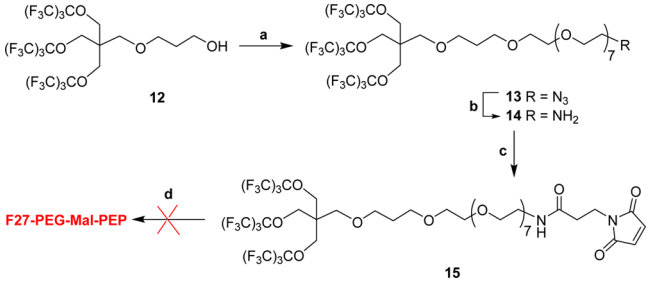

[a]Reagents and conditions: (a) compound **6**, NaH, THF, reflux; (b) Ph_3P, THF, then H_2O, rt; (c) 3-(maleimido)propionic acid, HOBT, EDC·HCl, DIPEA, DMF; (d) compound **10**, PBS/EtOH (v/v, 4/1), pH 7.4, rt.

MMP-2 substrate **10** via the sulfide–maleimide reaction. This reaction failed under the various conditions attempted. This difficulty could come from the strong hydrophobicity of compound **15**, which did not allow its dispersion/dissolvation into the aqueous media required for this coupling reaction.

***In Vitro* Studies: MMP-2 Specificity.** First we used the probe to detect activity of purified MMP-2. Probe **11** (0.25 mM) was incubated with MMP-2, and ^{19}F NMR was used to monitor the ^{19}F signal recovery at 37 °C over time. Time-dependent ^{19}F NMR spectra, including intensity and signal/noise ratio were recorded (Figure 2). Before adding MMP-2, ^{19}F signal exhibited a broad peak with full width at half the maximum (fwhm) of around 12.7 Hz due to the strong paramagnetic effect of Gd^{3+} toward ^{19}F. Upon MMP-2 incubation, ^{19}F signal started to increase at 15 min and an apparent sharp/signal appeared at 60 min, which further increased over time, until reaching a plateau at 17 h. The fwhm dropped to 2.1 Hz, and the ^{19}F intensity increased by 8.5-fold (Figure 3). Time-dependent signal/noise ratio of ^{19}F NMR showed the similar trend with ^{19}F intensity change. MMP-2 specificity of the probe was confirmed by coincubation with a

dx.doi.org/10.1021/mp500443x | *Mol. Pharmaceutics* 2014, 11, 4208–4217

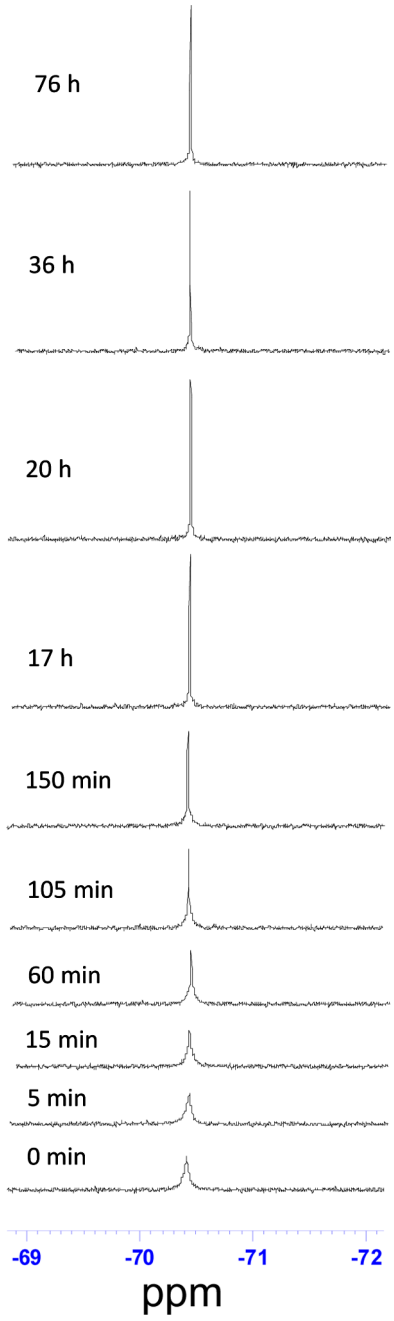

Figure 2. Time-dependent ^{19}F NMR spectral changes of F9-PEG-Mal-PEP-DOTA-Gd (0.25 mM) after adding MMP-2 (26.9 nM) at 37 °C. Reaction buffer: 50 mM Tris, 10 mM $CaCl_2$, 150 mM NaCl, 0.05% Brij35, pH 7.8, 5% D_2O.

broad spectrum pan-MMP inhibitor.[34,35] There was almost no change of ^{19}F intensity when MMP inhibitor (MMPI) was added to the system, indicating the substrate specificity. The fluorine signal and signal/noise ratio remained unchanged in blank buffer, suggesting that the fluorine signal recovery was induced by MMP specific cleavage. LC−MS further confirmed the site-specific cleavage of the peptide in the presence of MMP-2.

Secretive MMP-2 Activity Detection of Living Cells. With the purified MMP-2 activity evaluated, we further applied our probe for real-time monitoring of secreted MMP-2 activity in living cells. SCC7 cell line was chosen because these cells secrete a high level of MMP-2. Before the detection of MMP

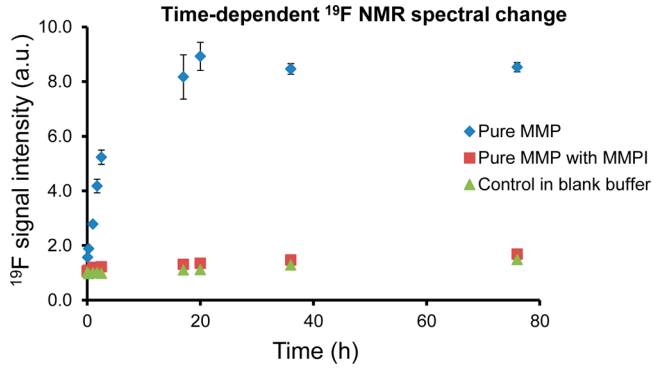

Figure 3. Recovery of ^{19}F signal in the presence of pure MMP, pure MMP with MMP inhibitor, and probe without MMP treatment (control in blank buffer). Probe concentration is 0.25 mM.

activity, an ELISA MMP assay kit was used to estimate the MMP concentration, and the level was found to be 8.5 ng/mL in cell culture medium. The newly synthesized ^{19}F probe was then incubated with the cell medium. The ^{19}F signal recovery was apparent at 60 min, and the signal reached a plateau at 36 h. Compared with pure MMP, the signal increased about 4.8-fold (Figure 4 and 5). In contrast, the ^{19}F signal only increased 1.9-fold in the presence of MMP-2 inhibitor, and no significant ^{19}F signal change was found when the probe was incubated with either blank buffer or pure water. Enzymes other than MMP-2 in the cell medium may also lead to nonspecific cleavage of the probe, which explains why MMP-2 inhibitor was unable to completely suppress ^{19}F signal.

Relaxation Time Determination. To further evaluate the MMP activity secreted by SCC7 cancer cells, we measured the longitudinal relaxation time T_1 and and transverse relaxation time T_2 of the ^{19}F signal under different conditions. The results showed that F9-PEG-Mal-PEP-DOTA substrate without Gd chelation exhibited long T_1 and T_2 with strong ^{19}F signal. In contrast, both T_1 and T_2 were significantly reduced after Gd^{3+} incorporation, indicating the strong paramagnetic effect of Gd^{3+} toward ^{19}F, which leads to over 20 times reduction of T_2 and broadening of ^{19}F signal. However, this effect was dissipated during the probe incubation in SCC7 conditioned medium, in which the T_1 and T_2 increased rapidly with significant ^{19}F signal recovery. This signal recovery was correlated with MMP-2 activity in the conditioned medium. Compared to Gd^{3+} free conditions, the T_1 and T_2 values of Gd^{3+} complex after incubation with cell medium did not fully recover. This might be due to the fact that Gd^{3+} is still in the solution, but that interaction is reduced due to an increased average distance between Gd^{3+} ions and ^{19}F atoms[28] (Table 1).

^{19}F MRI Imaging of MMP-2 Activity. ^{19}F MRI imaging was performed to show the ^{19}F signal intensity change upon treatment with SCC7 cell medium (Figure 6). Before SCC7 conditioned cell medium incubation, there was no ^{19}F imaging signal except for background noise. After incubation with conditioned medium overnight, the ^{19}F MRI was clearly visualized under the same fluorine concentration. The promising results further showed that our probe was able to visualize MMP activity.

DISCUSSION

MMPs play an important role in a series of normal physiological processes with low expression level. However, MMPs are overexpressed in numerous pathological diseases,

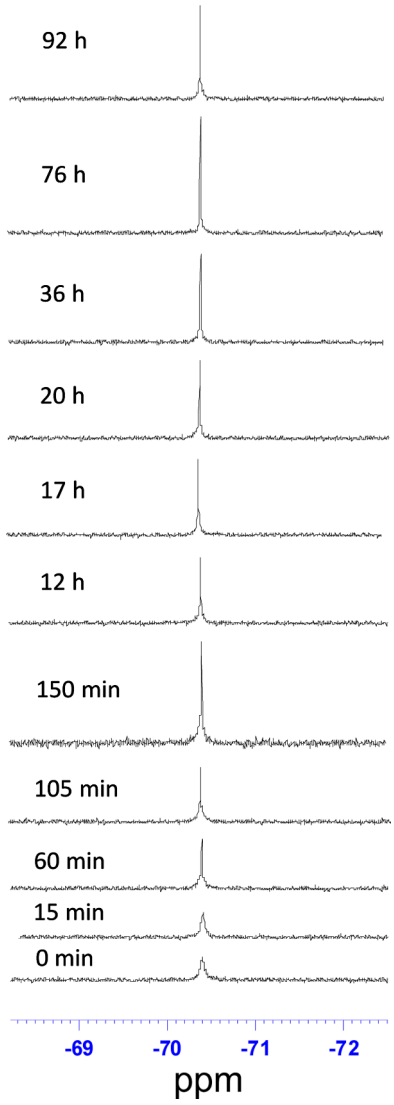

Figure 4. Time-dependent ^{19}F NMR spectral changes of F9-PEG-Mal-PEP-DOTA-Gd (0.25 mM) after the addition of SCC7 cell medium at 37 °C; MMP-2 concentration was 8.5 ng/mL determined by MMP assay kit.

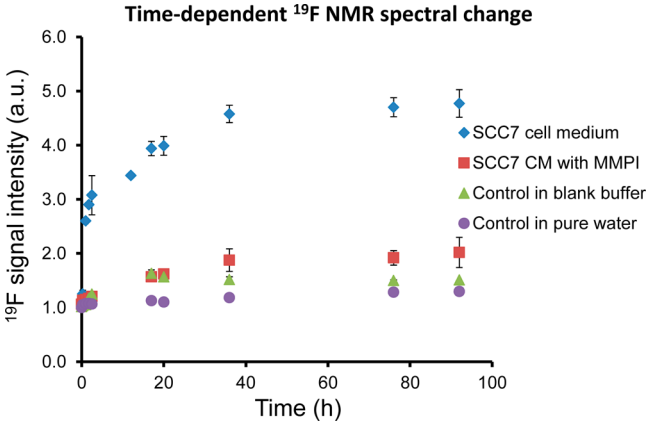

Figure 5. Recovery of ^{19}F signal in the presence of SCC7 cell medium, cell medium with MMP inhibitor treatment, and probe incubation in the presence of blank buffer or pure water. Probe concentration is 0.25 mM.

Table 1. T_1 and T_2 Change of Synthesized MMP Substrates before and after SCC7 Cell Medium Incubation

	T_1 (ms)	T_2 (ms)
F9-PEG-Mal-PEP-DOTA	1760	518
F9-PEG-Mal-PEP-DOTA-Gd	33.2	17.3
F9-PEG-Mal-PEP-DOTA-Gd + SCC7 cell medium	245.7	57.7

such as inflammation, and tumor metastasis. Noninvasive imaging of activated MMPs and other proteases has been extensively studied in recent years for tumor diagnosis. While optical imaging is the most used strategy for visualization of MMPs, its combination with iron oxide-based nanoformulation for multimodality imaging has received great attention.[19,20] Chen et al. designed an Au−Fe_3O_4 composite activatable nanoparticle by integrating the excellent quenching property of gold nanoparticle toward fluorescent dyes and easily tunable surface chemistry of iron oxide nanoparticle for imaging of MMPs with great success.[19] Kim et al. reported a MRI/NIRF-based dual modal imaging probe composed of silica-coated iron oxide nanoparticles and Cy5.5-MMP unit that can be visualized *in vivo* by both MRI and optical imaging.[20]

^{1}H MRI is extensively used clinically for diagnosis due to the high concentration of water in the human body (55 M).[36] Traditional anatomical ^{1}H MRI relies on signal from protons in water of tissues; contrast agents such as positive Gd-based[37,38] or negative iron oxide-based contrast agents[39] are used to enhance contrast. However, for metal-based contrast agents, image artifacts are sometimes produced due to the difficulty in discrimination between the targeted tissues and susceptibility associated with surrounding environment. ^{19}F MRI detects ^{19}F nuclei directly with negligible background and can be used for quantitative purpose in living subjects. The advancement of ^{19}F MRI has lagged behind that of ^{1}H MRI although ^{19}F was investigated early in the history of MRI.[40,41] Unlike the protons from water molecules, most fluorine compounds have non-equivalent fluorine atoms that spread the resonance signals through a relatively wide chemical shift range.

A series of ^{19}F-based activatable probes responsive to pH,[42,43] temperature,[44] enzymatic activity,[27,28] and redox potential[45] have been reported. Most of the developed probes contain a single trifluoromethyl group; thus, sensitivity is an issue in these model systems. Hence, increasing the number of fluorine atoms in a single molecule is one strategy to enhance the sensitivity of the ^{19}F probes. Hamachi et al. reported several ^{19}F-based self-assembling nanoprobes for protein detection. Results showed that the sensitivity of the designed probes is linear to the number of the incorporated fluorine atoms.[29] Our recently developed fluorous dendron-cyanine dye-conjugated nanoprobe successfully achieved optical/MR bimodal imaging *in vivo*.[46] Here we described a set of MMP-responsive probes with highly symmetrical fluorinated branches, which exhibited a single/sharp resonance with negligible chemical shift change during incubation with enzyme. Perfluorocarbon-based imaging agents, including emulsions and polymers, usually exhibit split ^{19}F resonance, and may cause imaging artifacts.[32] PFCE with highly symmetric fluorine atoms and considerable fluorine content makes it the most commonly used fluorous agent in ^{19}F MRI, but PFCE is insoluble in almost all solvents and is not amenable to chemical modifications. Complex formulation procedures are required for imaging purposes. Compared to PFCE and other perfluorocarbon-based imaging agents, our probe exhibited highly symmetric signal emitter, and the

dx.doi.org/10.1021/mp500443x | *Mol. Pharmaceutics* 2014, 11, 4208−4217

Figure 6. ^{19}F imaging of a solution (2.5 mM) of probe **11** before (left) and after (middle) SCC7 cell medium incubation. As a control, a solution (right) of F9-PEG-Mal-PEP-DOTA without Gd^{3+} incorporation was also imaged. The experiments were performed with a homemade surface coil tuned to 281.65 MHz, which is the ^{19}F resonance frequency at 7 T. A 2D FLASH image was acquired on the probe, with the following acquisition parameters: TE = 3 ms, TR = 100 ms, FOV = 4 × 4 cm^2, matrix size = 128 × 128, slice thickness = 2 mm, and FA = 30 deg.

fluorine content was easily tunable. In addition, water solubility was modulatable by switching the length of PEGylated chain or the number of symmetric fluorine branches.

Extensive studies of ^{19}F MRI in recent years have pointed out the comparatively low sensitivity observed when compared to ^{1}H MRI.[36,41] Our activatable probe encountered similar issue since millimolar concentration was required to provide enough ^{19}F signal to visualize MMP activity. Further advances in both instrumentation and chemistry, such as increasing the number of equivalent fluorine in the probe design for higher sensitivity,[26] are required to improve the detection limit. Compared to iron oxide nanoparticles, ^{19}F MRI is able to quantitatively evaluate MMP level with low background noise, but the sensitivity of ^{19}F MRI agent is lower than iron oxide nanoparticles. Especially for clinical translation, the sensitivity of ^{19}F MRI remains a challenge because local ^{19}F concentration at the target site is far below the ^{1}H level in the human body. The use of higher dose of ^{19}F agents for clinical application may provide better sensitivity, assuming target uptake correlates with dose, but introduces the potential trade-off between sensitivity and toxicity for regulatory approval. However, PFC based imaging agents have been approved for a clinical trial in the US.[30] Another challenge would be the selectivity and specificity of the probe for protease detection due to considerable concentration of MMP-2/MMP-9 in atherosclerotic vessels, major arteries, and microvasculature. The developed probe needs to be sensitive enough to discriminate the target pathological site. By appropriate installation of symmetrical fluorine branches and tuning the substrate to different targets, we may use this strategy to image other enzymatic pathology *in vivo*.

■ CONCLUSIONS

In conclusion, a fluorous probe was developed to detect MMP activity of living cells. The probe features a highly symmetrical fluorine signal emitting unit, with a remarkable time-dependent fluorine signal recovery upon incubation with MMP-2 enzyme, indicating that our probe is capable of specifically monitoring MMP-2 activity in real-time. Our reported ^{19}F-based probe can be widely used to detect enzyme activities by properly changing the substrate structures. This symmetrical fluorine dendron-based probe design extends the scope of existing ^{19}F MRI agents and provides another simple but robust method for real-time ^{19}F MRI application.

■ AUTHOR INFORMATION

Corresponding Authors

*(D.O.K.) E-mail: dkiesewetter@mail.nih.gov

*(X.C.) E-mail: shawn.chen@nih.gov

Present Address

#(X.Y.) Department of Radiology, Washington University School of Medicine, St. Louis, Missouri 63110, United States.

Author Contributions

⊥X.Y. and Z.W. contributed equally to this work.

Notes

The authors declare no competing financial interest.

■ ACKNOWLEDGMENTS

This work was supported by the intramural research program of the National Institute of Biomedical Imaging and Bioengineering, National Institutes of Health, and the National Science Foundation of China (NSFC) (81301256).

■ REFERENCES

(1) Massova, I.; Kotra, L. P.; Fridman, R.; Mobashery, S. Matrix metalloproteinases: structures, evolution, and diversification. *FASEB J.* **1998**, *12* (12), 1075−95.

(2) Nagase, H.; Woessner, J. F., Jr. Matrix metalloproteinases. *J. Biol. Chem.* **1999**, *274* (31), 21491−4.

(3) Folgueras, A. R.; Pendas, A. M.; Sanchez, L. M.; Lopez-Otin, C. Matrix metalloproteinases in cancer: from new functions to improved inhibition strategies. *Int. J. Dev. Biol.* **2004**, *48* (5−6), 411−24.

(4) Galis, Z. S.; Khatri, J. J. Matrix metalloproteinases in vascular remodeling and atherogenesis: the good, the bad, and the ugly. *Circ. Res.* **2002**, *90* (3), 251−62.

(5) Bauvois, B. New facets of matrix metalloproteinases MMP-2 and MMP-9 as cell surface transducers: outside-in signaling and relationship to tumor progression. *Biochim. Biophys. Acta* **2012**, *1825* (1), 29−36.

(6) Klein, G.; Vellenga, E.; Fraaije, M. W.; Kamps, W. A.; de Bont, E. S. The possible role of matrix metalloproteinase (MMP)-2 and MMP-9 in cancer, e.g. acute leukemia. *Crit. Rev. Oncol. Hematol.* **2004**, *50* (2), 87−100.

(7) Curran, S.; Murray, G. I. Matrix metalloproteinases in tumour invasion and metastasis. *J. Pathol.* **1999**, *189* (3), 300−8.

(8) Zucker, S.; Hymowitz, M.; Conner, C.; Zarrabi, H. M.; Hurewitz, A. N.; Matrisian, L.; Boyd, D.; Nicolson, G.; Montana, S. Measurement of matrix metalloproteinases and tissue inhibitors of metalloproteinases in blood and tissues. Clinical and experimental applications. *Ann. N.Y. Acad. Sci.* **1999**, *878*, 212−27.

(9) Lee, S. W.; Song, K. E.; Shin, D. S.; Ahn, S. M.; Ha, E. S.; Kim, D. J.; Nam, M. S.; Lee, K. W. Alterations in peripheral blood levels of TIMP-1, MMP-2, and MMP-9 in patients with type-2 diabetes. *Diabetes Res. Clin. Pract.* **2005**, *69* (2), 175−9.

(10) Maxwell, P. R.; Timms, P. M.; Chandran, S.; Gordon, D. Peripheral blood level alterations of TIMP-1, MMP-2 and MMP-9 in patients with type 1 diabetes. *Diabet. Med.* **2001**, *18* (10), 777−80.
(11) DeLano, F. A.; Schmid-Schonbein, G. W. Proteinase activity and receptor cleavage: mechanism for insulin resistance in the spontaneously hypertensive rat. *Hypertension* **2008**, *52* (2), 415−23.
(12) Friese, R. S.; Rao, F.; Khandrika, S.; Thomas, B.; Ziegler, M. G.; Schmid-Schonbein, G. W.; O'Connor, D. T. Matrix metalloproteinases: discrete elevations in essential hypertension and hypertensive end-stage renal disease. *Clin. Exp. Hypertens.* **2009**, *31* (7), 521−33.
(13) Zhang, Z.; Fan, J.; Cheney, P. P.; Berezin, M. Y.; Edwards, W. B.; Akers, W. J.; Shen, D.; Liang, K.; Culver, J. P.; Achilefu, S. Activatable molecular systems using homologous near-infrared fluorescent probes for monitoring enzyme activities in vitro, in cellulo, and in vivo. *Mol. Pharmaceutics* **2009**, *6* (2), 416−27.
(14) Zhu, L.; Zhang, F.; Ma, Y.; Liu, G.; Kim, K.; Fang, X.; Lee, S.; Chen, X. In vivo optical imaging of membrane-type matrix metalloproteinase (MT-MMP) activity. *Mol. Pharmaceutics* **2011**, *8* (6), 2331−8.
(15) Cai, Y.; Zhu, L.; Zhang, F.; Niu, G.; Lee, S.; Kimura, S.; Chen, X. Noninvasive monitoring of pulmonary fibrosis by targeting matrix metalloproteinases (MMPs). *Mol. Pharmaceutics* **2013**, *10* (6), 2237−47.
(16) Deguchi, J. O.; Aikawa, M.; Tung, C. H.; Aikawa, E.; Kim, D. E.; Ntziachristos, V.; Weissleder, R.; Libby, P. Inflammation in atherosclerosis: visualizing matrix metalloproteinase action in macrophages in vivo. *Circulation* **2006**, *114* (1), 55−62.
(17) Ibarra, J. M.; Jimenez, F.; Martinez, H. G.; Clark, K.; Ahuja, S. S. MMP-Activated fluorescence imaging detects early joint inflammation in collagen-antibody-induced arthritis in CC-chemokine receptor-2-null mice *in vivo*. *Int. J. Inflammation* **2011**, *2011*, 691587.
(18) Matsumura, S.; Aoki, I.; Saga, T.; Shiba, K. A tumor-environment-responsive nanocarrier that evolves its surface properties upon sensing matrix metalloproteinase-2 and initiates agglomeration to enhance T_2 relaxivity for magnetic resonance imaging. *Mol. Pharmaceutics* **2011**, *8* (5), 1970−4.
(19) Xie, J.; Zhang, F.; Aronova, M.; Zhu, L.; Lin, X.; Quan, Q.; Liu, G.; Zhang, G.; Choi, K. Y.; Kim, K.; Sun, X.; Lee, S.; Sun, S.; Leapman, R.; Chen, X. Manipulating the power of an additional phase: a flower-like Au-Fe_3O_4 optical nanosensor for imaging protease expressions in vivo. *ACS Nano* **2011**, *5* (4), 3043−51.
(20) Cha, E. J.; Jang, E. S.; Sun, I. C.; Lee, I. J.; Ko, J. H.; Kim, Y. I.; Kwon, I. C.; Kim, K.; Ahn, C. H. Development of MRI/NIRF 'activatable' multimodal imaging probe based on iron oxide nanoparticles. *J. Controlled Release* **2011**, *155* (2), 152−8.
(21) Ansari, C.; Tikhomirov, G. A.; Hong, S. H.; Falconer, R. A.; Loadman, P. M.; Gill, J. H.; Castaneda, R.; Hazard, F. K.; Tong, L.; Lenkov, O. D.; Felsher, D. W.; Rao, J.; Daldrup-Link, H. E. Development of novel tumor-targeted theranostic nanoparticles activated by membrane-type matrix metalloproteinases for combined cancer magnetic resonance imaging and therapy. *Small* **2014**, *10* (3), 566−75 417..
(22) Gallo, J.; Kamaly, N.; Lavdas, I.; Stevens, E.; Nguyen, Q. D.; Wylezinska-Arridge, M.; Aboagye, E. O.; Long, N. J. CXCR4-targeted and MMP-responsive iron oxide nanoparticles for enhanced magnetic resonance Imaging. *Angew. Chem., Int. Ed.* **2014**, *53*, 9550−9554.
(23) Huang, C. W.; Li, Z.; Conti, P. S. Radioactive smart probe for potential corrected matrix metalloproteinase imaging. *Bioconjugate Chem.* **2012**, *23* (11), 2159−67.
(24) van Duijnhoven, S. M.; Robillard, M. S.; Hermann, S.; Kuhlmann, M. T.; Schafers, M.; Nicolay, K.; Grull, H. Imaging of MMP activity in postischemic cardiac remodeling using radiolabeled MMP-2/9 activatable peptide probes. *Mol. Pharmaceutics* **2014**, *11* (5), 1415−23.
(25) Chuang, C. H.; Chuang, K. H.; Wang, H. E.; Roffler, S. R.; Shiea, J. T.; Tzou, S. C.; Cheng, T. C.; Kao, C. H.; Wu, S. Y.; Tseng, W. L.; Cheng, C. M.; Hou, M. F.; Wang, J. M.; Cheng, T. L. In vivo positron emission tomography imaging of protease activity by generation of a hydrophobic product from a noninhibitory protease substrate. *Clin. Cancer Res.* **2012**, *18* (1), 238−47.
(26) Matsuo, K.; Kamada, R.; Mizusawa, K.; Imai, H.; Takayama, Y.; Narazaki, M.; Matsuda, T.; Takaoka, Y.; Hamachi, I. Specific detection and imaging of enzyme activity by signal-amplifiable self-assembling ^{19}F MRI probes. *Chemistry* **2013**, *19* (38), 12875−83.
(27) Mizukami, S.; Takikawa, R.; Sugihara, F.; Shirakawa, M.; Kikuchi, K. Dual-function probe to detect protease activity for fluorescence measurement and ^{19}F MRI. *Angew. Chem., Int. Ed.* **2009**, *48* (20), 3641−3.
(28) Mizukami, S.; Takikawa, R.; Sugihara, F.; Hori, Y.; Tochio, H.; Walchli, M.; Shirakawa, M.; Kikuchi, K. Paramagnetic relaxation-based ^{19}F MRI probe to detect protease activity. *J. Am. Chem. Soc.* **2008**, *130* (3), 794−5.
(29) Takaoka, Y.; Kiminami, K.; Mizusawa, K.; Matsuo, K.; Narazaki, M.; Matsuda, T.; Hamachi, I. Systematic study of protein detection mechanism of self-assembling ^{19}F NMR/MRI nanoprobes toward rational design and improved sensitivity. *J. Am. Chem. Soc.* **2011**, *133* (30), 11725−31.
(30) Ahrens, E. T.; Bulte, J. W. Tracking immune cells in vivo using magnetic resonance imaging. *Nat. Rev. Immunol.* **2013**, *13* (10), 755−63.
(31) Schmieder, A. H.; Wang, K.; Zhang, H.; Senpan, A.; Pan, D.; Keupp, J.; Caruthers, S. D.; Wickline, S. A.; Shen, B.; Wagner, E. M.; Lanza, G. M. Characterization of early neovascular response to acute lung ischemia using simultaneous $^{19}F/^{1}H$ MR molecular imaging. *Angiogenesis* **2014**, *17* (1), 51−60.
(32) Srinivas, M.; Cruz, L. J.; Bonetto, F.; Heerschap, A.; Figdor, C. G.; de Vries, I. J. Customizable, multi-functional fluorocarbon nanoparticles for quantitative in vivo imaging using ^{19}F MRI and optical imaging. *Biomaterials* **2010**, *31* (27), 7070−7.
(33) Yue, X. Y.; Taraban, M. B.; Hyland, L. L.; Yu, Y. B. Avoiding steric congestion in dendrimer growth through proportionate branching: A twist on da Vinci's rule of tree branching. *J. Org. Chem.* **2012**, *77* (20), 8879−8887.
(34) Corcoran, M. L.; Hewitt, R. E.; Kleiner, D. E., Jr.; Stetler-Stevenson, W. G. MMP-2: expression, activation and inhibition. *Enzyme Protein* **1996**, *49* (1−3), 7−19.
(35) Ikejiri, M.; Bernardo, M. M.; Bonfil, R. D.; Toth, M.; Chang, M.; Fridman, R.; Mobashery, S. Potent mechanism-based inhibitors for matrix metalloproteinases. *J. Biol. Chem.* **2005**, *280* (40), 33992−4002.
(36) Wolters, M.; Mohades, S. G.; Hackeng, T. M.; Post, M. J.; Kooi, M. E.; Backes, W. H. Clinical perspectives of hybrid proton-fluorine magnetic resonance imaging and spectroscopy. *Invest. Radiol.* **2013**, *48* (5), 341−50.
(37) Neubauer, A. M.; Myerson, J.; Caruthers, S. D.; Hockett, F. D.; Winter, P. M.; Chen, J. J.; Gaffney, P. J.; Robertson, J. D.; Lanza, G. M.; Wickline, S. A. Gadolinium-modulated F-19 signals from perfluorocarbon nanoparticles as a new strategy for molecular imaging. *Magn. Reson. Med.* **2008**, *60* (5), 1066−1072.
(38) de Vries, A.; Moonen, R.; Yildirim, M.; Langereis, S.; Lamerichs, R.; Pikkemaat, J. A.; Baroni, S.; Terreno, E.; Nicolay, K.; Strijkers, G. J.; Grull, H. Relaxometric studies of gadolinium-functionalized perfluorocarbon nanoparticles for MR imaging. *Contrast Media Mol. Imaging* **2014**, *9* (1), 83−91.
(39) Nie, L.; Wang, S.; Wang, X.; Rong, P.; Ma, Y.; Liu, G.; Huang, P.; Lu, G.; Chen, X. In vivo volumetric photoacoustic molecular angiography and therapeutic monitoring with targeted plasmonic nanostars. *Small* **2014**, *10* (8), 1585−93.
(40) Lanza, G. M.; Winter, P. M.; Neubauer, A. M.; Caruthers, S. D.; Hockett, F. D.; Wickline, S. A. $^{1}H/^{19}F$ magnetic resonance molecular imaging with perfluorocarbon nanoparticles. *Curr. Top. Dev. Biol.* **2005**, *70*, 57−76.
(41) Chen, J.; Lanza, G. M.; Wickline, S. A. Quantitative magnetic resonance fluorine imaging: today and tomorrow. *Wiley Interdiscip. Rev.: Nanomed. Nanobiotechnol.* **2010**, *2* (4), 431−40.
(42) Huang, X.; Huang, G.; Zhang, S.; Sagiyama, K.; Togao, O.; Ma, X.; Wang, Y.; Li, Y.; Soesbe, T. C.; Sumer, B. D.; Takahashi, M.; Sherry, A. D.; Gao, J. Multi-chromatic pH-activatable ^{19}F-MRI

nanoprobes with binary ON/OFF pH transitions and chemical-shift barcodes. *Angew. Chem., Int. Ed.* **2013**, *52* (31), 8074−8.
(43) Oishi, M.; Sumitani, S.; Nagasaki, Y. On-off regulation of ^{19}F magnetic resonance signals based on pH-sensitive PEGylated nanogels for potential tumor-specific smart ^{19}F MRI probes. *Bioconjugate Chem.* **2007**, *18* (5), 1379−82.
(44) Kitamura, N.; Tanaka, K.; Chujo, Y. Heat-initiated detection for reduced glutathione with ^{19}F NMR probes based on modified gold nanoparticles. *Bioorg. Med. Chem. Lett.* **2013**, *23* (1), 281−6.
(45) Tanaka, K.; Kitamura, N.; Takahashi, Y.; Chujo, Y. Reversible signal regulation system of ^{19}F NMR by redox reactions using a metal complex as a switching module. *Bioorg. Med. Chem.* **2009**, *17* (11), 3818−23.
(46) Wang, Z.; Yue, X.; Wang, Y.; Qian, C.; Huang, P.; Lizak, M.; Niu, G.; Wang, F.; Rong, P.; Kiesewetter, D. O.; Ma, Y.; Chen, X. A symmetrical fluorous dendron-cyanine dye conjugated bimodal nanoprobe for quantitative ^{19}F MRI and NIR fluorescence bioimaging. *Adv. Healthcare Mater.* **2014**, *3* (8), 1326−33.